Delineation of ore zones using the concentration-volume fractal method in the Dagh Dali Zn-Pb (±Au) prospect, north of Takab (Iran)

Zahra Yekani MOTLAGH[1], Ali IMAMALIPOUR[1, *] and Habibollah BAZDAR[1]

[1] Urmia University, Department of Mining Engineering, 57153-165 Urmia, Islamic Republic of Iran

The Dagh Dali Zn-Pb (±Au) hydrothermal prospect is located in the north-west of Iran. Identification of mineralized zones is essential in ore deposit exploration. Different methods have been developed and applied to separate mineralized zones from barren host rocks based on mineralogical and petrographical studies, alteration and host rock changes as well as statistical and geostatistical parameters. This study uses the ordinary kriging technique and the concentration-volume fractal (C-V) method to model the ore body and recognize the ore grade distribution. These techniques were applied on the drillcore data and C-V fractal modelling, values of various ore zones being determined. Four breakpoints were found in the log-log plots which correspond to concentrations of 5.4, 10.5, and 17.8 wt.% Zn. The extractable ore zone for Zn is considered to be in the concentration range of 5.4 to 17.8 wt.%. Compared to the amount of reserve obtained from the geostatistical method (303,685 tons), it seems that the fractal method is more precise and accurate in the estimation of ore reserves.

Key words: Ore zone, concentration-volume (C-V) fractal method, Kriging, *Micromine* software, Dagh Dali.

INTRODUCTION

Fractal geometry is a branch of non-linear mathematics that has been widely used in different fields of geoscience since the 1980s. Noting that classical Euclidean geometry is not practical in explaining the true geometry of natural objects, scientists have sought to determine a geometry which is able to describe irregular and complex elements in nature (Davis, 2002). For this purpose, the concept of fractal geometry was introduced by Mandelbrot (1983). In fractal geometry, each shape and its complexities are represented in the form of numbers, whilst in Euclidean geometry, the concepts of angle, length, area, and one-dimensional space are used in up to three dimensions. In fractal geometry, there are fractal dimensions that are normally not integer numbers and that are called fractal pixels, which can be used to express the complexity of a shape.

In geochemical exploration, the fractal method was first used to quantitatively figure out anomalous thresholds and to separate geochemical anomalies from background values, which is crucial in exploration geochemistry (Cheng et al., 1997; Bai et al., 2010). The traditional statistical methods which are

used in the interpretion of geochemical data are not able to statistically analyse the concentration of elements when they are in the form of normal or log-normal patterns in the Earth crust. Therefore, the traditional methods are based on the frequency distribution of geochemical concentrations without considering their geometrical and spatial variation (Li et al., 2003). However, element concentrations do vary spatially, and this encourages new methods for detecting geochemical anomalies associated with mineralisation that can exploit such spatial variation. Consequently, many different space-based methods have been proposed for geochemical landscape studies, based on the spatially-dependent characteristics of geochemical data, and various studies have considered the potential of fractal modelling in geochemical exploration (Cheng et al., 1994; Carranza, 2008). Hence, different methods of fractal modelling have been introduced during the 1980s and 1990s including the concentration-area (C-A) model (Cheng et al., 1994) the concentration-distance (C-D) model (Li et al., 2003), the concentration-perimeter model and the spectrum-area model (S-A) (Cheng et al., 1999). Application of the concentration-area method has been widely developed in the field of earth sciences (Davis, 2002).

Nowadays, separation and identification of low-concentration and high-concentration zones in vein-type ore deposits are receiving attention. Using C-V fractal modelling, we can determine the area of the ore and identify the mineral zones. Fractal methods can be used to describe the relationships between geological, geochemical and mineralogical settings with spatial

information derived from analysis of mineral deposit occurrence data (Gonçalves et al., 2001; Carranza, 2008; Carranza et al., 2009; Afzal et al., 2011). However, a good knowledge of geological and geochemical environmental controls on mineralisation is essential for recognition and classification of geochemical populations based on methods of fractal analysis (Cheng, 1999; Sim et al., 1999; Gonçalves et al., 2001; Li et al., 2003; Carranza, 2009; Carranza and Sadeghi, 2010). The C-V fractal method is an accurate tool to distinguish between low-concentration and high-concentration ore zones. This method is based on the relation between the element concentration and the volume which includes the element concentration. Accordingly, by increasing the concentration, the volume containing that concentration will be reduced. This means that they are inversely related to each other (Afzal et al., 2013). Various log-log plots in fractal methods are appropriate tools for separation of geochemical populations. Extreme tilt variations in the C-V log-log plots indicate major changes in geological and mineralogical populations (Sadeghi et al., 2012). In the other words, quantitative threshold values can be determined in the plot's breakpoints, representing mineralisation zones. The main advantage of the C-V fractal method as compared to other traditional methods is the attention paid to fractal geometry, which is the natural geometry of the ore, and also in considering the concentration and the volume containing that concentration, which can be used to separate high-concentration veins from other veins (Cheng, 2007; Afzal et al., 2010, 2011). A number of studies have been carried out to separate different mineralisation zones. The first modelling aimed at recognition of ore zones was conducted on the San Manuel Santa Cruz porphyry copper deposit in Arizona (USA) (Lowell and Guilbert, 1970). In this model, potassic, phyllic and propylitic alteration zones were recognized in a monzonite type deposit. This deposit is characterized by well-defined alteration zoning. A major problem in this model is the lack of attention to element or main element concentrations in the porphyry deposits. Zuo et al. (2009) initially introduced the vertical distribution of elements and its importance to extraction planning, and applied fractal-based methods at deep levels for the first time. Geochemical data have multifractal behaviour in general, which reflect changes in geological, geochemical, alteration, surface weathering and mineralisation conditions as well as the enrichment stages of an element (Gonçalves et al., 2001).

The purpose of this study is to identify different ore zones in the Dagh Dali prospect using the C-V fractal method, based on the distribution of Zn concentrations in boreholes. Modelling of the ore was first performed by the ordinary kriging method and then concentration-volume fractal modelling was applied to the orebody. Ore reserve was calculated by these two methods and the results were compared.

GEOLOGICAL SETTING

The Zn-Pb prospect of Dagh Dali is situated in the Takab region in the north-west of Iran (Fig. 1). Geographically, this area is located at 47°04'35"–47°08'27"E longitude and 36°43'11–36°46'26"N latitude. Takab is interesting from both structural and metallogenic points of view. Geologically and structurally, this region is closely related to Central Iran in some aspects and resembles Alborz and Sanandaj-Sirjan in other aspects (Ghorbani, 2013). Takab area lies at the boundary between the Urumieh-Dokhtar Magmatic Arc (UDMA) and the Sanandaj-Sirjan metamorphic zone (SSZ). This is a suture zone resulting from closure of the Neo-Tethyan Ocean and its

subsequent continental collision (Alavi, 1994). The principal structure at a regional scale is the NNW-trending Geynardjeh Thrust (a subsidiary of the Zagros Thrust), along which the Angouran Block has been thrust westwards onto the Takab Basin (also called the Shirmard Basin; Daliran, 2008).

The area has experienced repeated cycles of orogenic activity, including structural uplift, sedimentation, magmatism and metamorphism (Alavi et al., 1982). Igneous, sedimentary and metamorphic rocks ranging in age from Upper Precambrian to Quaternary outcrop in the Takab region. Stratigraphically, the rocks belonging to the Upper Precambrian-Lower Cambrian and Oligocene-Miocene intervals show the greatest areal distribution and lithological variation (Ghorbani, 2013). The lithostratigraphic sequence in the region starts with the Upper Precambrian Kahar schists and ends in the Miocene upper redbed successions. The Lower Red Formation, comprising a transgressive continental redbed sequence of basal conglomerate, sandstone and marl along with evaporitic deposits, directly overlies the basement rocks and is Oligocene in age (Alavi et al., 1982; Daliran, 2008). Thick dolomitic limestone of the Jangortaran Formation overlies the Precambrian schists. These two lithostratigraphic units are located in the eastern part of the study area and have been strongly altered by tectonic-hydrothermal processes in this zone. The main mineralisation events leading to Au, As, Zn, and Pb ores occurred within these rocks. In this area, volcanic activity occurred during the Late Precambrian, Cretaceous, Eocene, Oligo-Miocene, and after the Miocene. Neogene volcano-plutonic rocks including rhyolites, basalts, and tuffs along with small intrusions of gabbro and alkali granite cover ~30% of the area (Asadi and Hale, 2001). These igneous events were followed by intense hydrothermal processes which are still active in the form of thermal springs (Ghorbani, 2013). Thermal springs have resulted in the formation of numerous dissected travertine outcrops in this area. The hot springs are commonly controlled by faults such as the intersection of NE-, NW- and E-trending faults at Takht-e- (or Zendan-e-) Soleyman (Daliran, 2008).

A series of geological events, during the two separate intervals of Late Precambrian–Early Cambrian and Neogene, have made Takab one of the most important metallogenic provinces in the country (Ghorbani, 2013), particularly in terms of the mineralisation of Au, Pb and Zn. The two well-known Au deposits of Zarshuran and Agh Darreh and the largest Pb and Zn deposit of Iran (Anguran) along with some other important deposits are located in this zone.

MINERALISATION

The Dagh Dali mineralisation zone is located in the vicinity of the Zarshuran Au deposit, a major ore deposit of Iran. This region hosts an active geothermal field where thermal springs locally precipitate considerable amounts of Au and Ag, up to kg/t level. Fault-hosted, vein and disseminated sediment-hosted deposits of Au, As, and Sb in Takab are associated with thermal springs and numerous dissected outcrops of travertine up to 100 km^2 in area (Daliran, 2003, 2008). Several small mineral occurrences also occur in this region including deposits of As-Au (Arabshah), Sb (Agh Darreh Bala, Balderghani, Bakhair--Bolaghi), Hg (Shirmard, Yar Aziz, Shakh-Shakh Mountain), Mn (Dabal Kuh), Fe (Shahrak, Kuh Baba), Pb-Zn (Ay Ghalasi, Arpachay) and Zn (Au-Fe) (Chichaklou) (Daliran, 2008).

There are also a number of less significant prospects of arsenic, antimony and gold in the vicinity of Zarshuran and Agh Darreh (Asadi and Hale, 2001; Fig. 2). The Dagh Dali area,
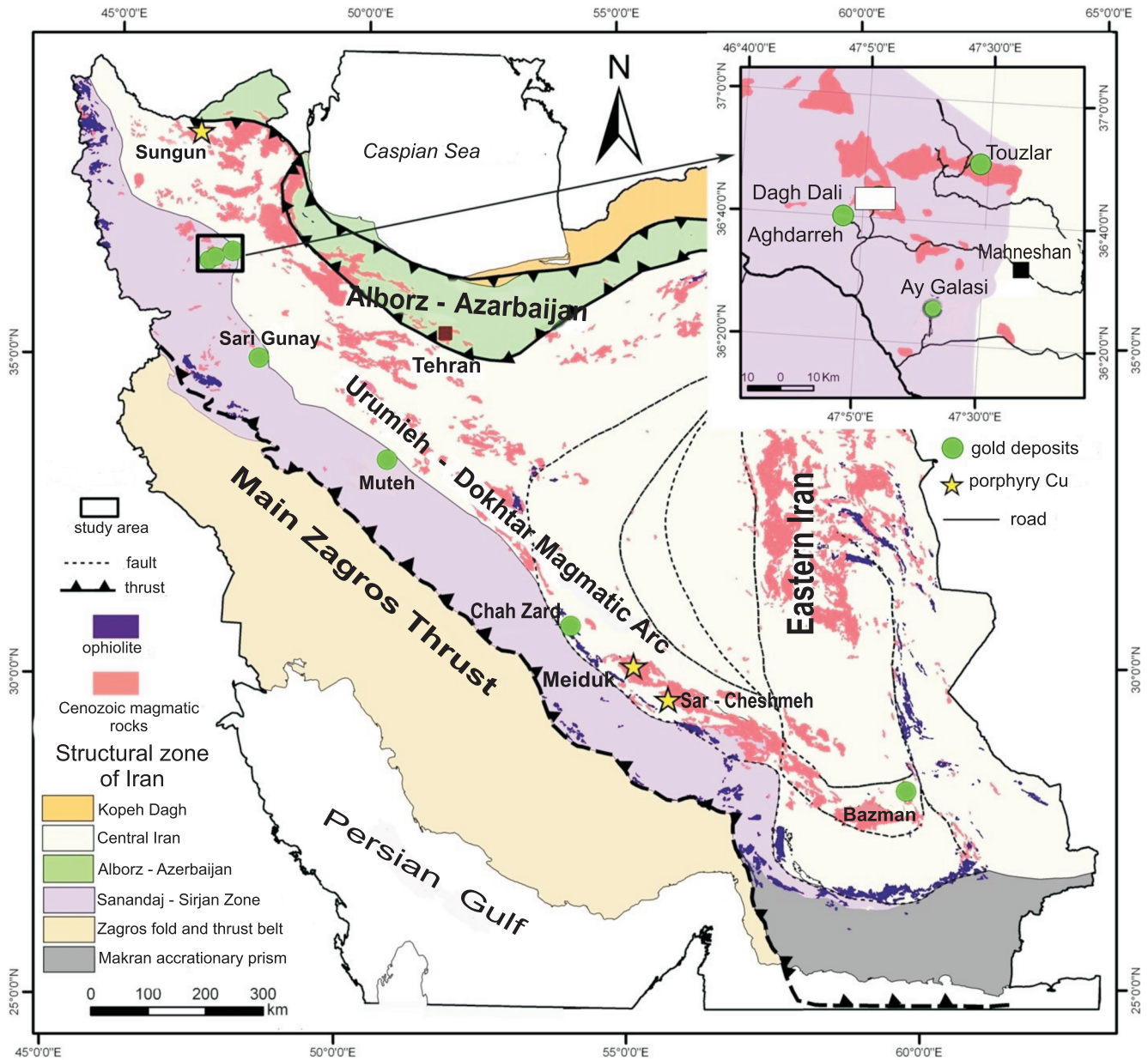
Fig. 1. Major tectonic trends in Iran (modified after Stöcklin, 1968; Daliran, 2008) and location of the study area (Dagh Dali Zn-Au prospect) in northwestern Iran

~3 km north-west of Zarshuran, is one of these prospects. This area is composed of three mineralisation zones, namely Bakhair-Bolaghi, the middle zone and Baldir-Ghanee. The Bikhair-Bolaghi alteration zone is characterized by an east--west-trending extension which extends for 800 m in length and 200 m in width. Several indications of antimony mineralisation in the carbonate rocks of this zone have been reported, which are intruded by altered Oligo-Miocene andesite dikes (Karimi, 1993). This alteration zone with a distinct brown colour is easily identified in the field. Sinter type silicification is an important form of alteration in this zone. As, Zn and Au mineralisation has occurred at the contact of the Kahar schists and the altered dolomitic limestone of the Jangotaran Formation, which is controlled by silicified veins, restricted to shear zones. It is associated with disseminated and open-space filling mineralisation of galena, sphalerite, pyrite and chalcopyrite. Sphalerite, more abundant than galena, is mainly associated with galena or surrounded by pyrite. Galena is formed either as fine disseminated crystals in association with chalcopyrite or as massive deposits in association with sphalerite. A scanning study has shown an insignificant concentration of gold in the pyrite (Rahimsouri et al., 2019). Some siliceous veins containing realgar and stibnite have been found in sandstone and tuff of the Qom Formation. Silicification and argillic alteration comprise the main alteration types associated with mineralisation in the region. Fe-hydroxides are widespread in the mineralisation zones.

It has been suggested that the mineralisation in Dagh Dali area resembles the hydrothermal mineralisation system of the
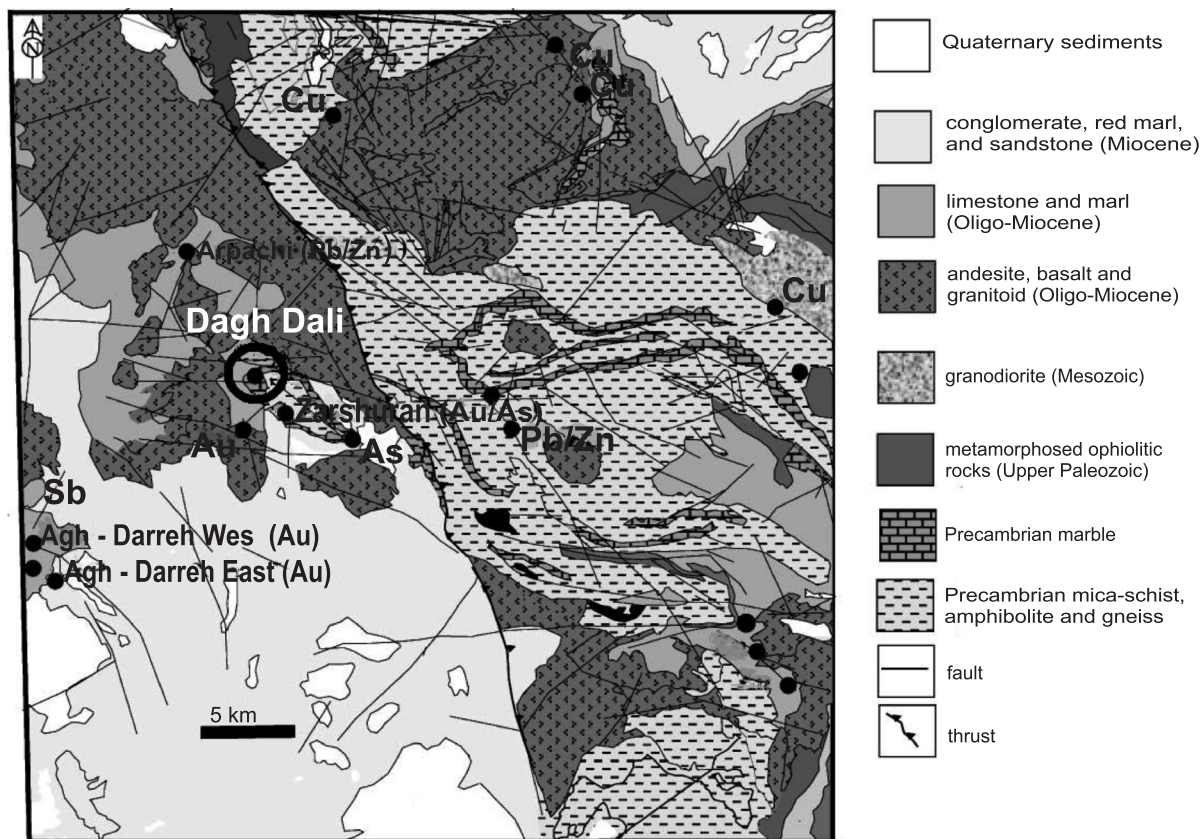
Fig. 2. Geological and mineral occurrence map of the Takab area (Asadi and Hale, 2001); the Dagh Dali occurrence
is located to the north-west of the Zarshuran Au mine

Zarshuran deposit which is to a large extent similar to the Carlin-type sediment-hosted Au deposits of the western United States (Asadi and Hale, 1999). From field observations and mineralogical and geochemical studies it was concluded that the mineralisation in the Dagh Dali prospect is hydrothermal in origin and is related to the Zarshuran mineralisation system. Fluid inclusion studies showed an ore-bearing fluid salinity of 4.55 to 6.81 wt.% NaCl eq., with a mean temperature of 212.5°C for Bekhair-Bolaghi and 1.65 to 10.48 wt.% NaCl eq. with temperatures between 170 to 207°C for Baldirghani. Based on geological, mineralogical, geochemical and fluid inclusion studies, it was suggested that the Dagh Dali Zn-Pb deposit shows similarities with low sulphidation type deposits (Rahimsouri et al., 2019).

The content of Zn varies widely between 43 and 244,000 ppm resulting in a high standard deviation of 25.851 ppm. Concentration of Au ranges from 10 to 560 ppb. The average Zn grade in the core samples studied is 3.70%. Based on the ore reserve calculation obtained by classical methods, the Dagh Dali prospect contains 521,181 Mt of ore reserves. Data on the Au grade is incomplete, determination of its mean grade requiring further investigation.

MATERIAL AND METHODS

Some exploratory operations were conducted in the Dagh Dali prospect by the Poya Zarkan Agh Darreh Company. In total, 2211 m has been diamond-drilled around the Dagh Dali prospect. In this study, data obtained from 49 exploratory boreholes are used. The distribution of boreholes is not perfectly regular, while the horizontal distance between boreholes is ~30 m.

Borehole locations are shown in Figure 3. This data includes geological logging and geochemical analysis of core samples. On average, samples were taken every 2 m, 2196 samples being collected. Each 2 m-length of core was split and one-half was selected for sample preparation. The samples were crushed, reduced in volume and pulverized to 200 mesh size. Samples were then divided into two fractions. One fraction of each sample was sent to the Acme Laboratory, Canada, where geochemical analysis of samples for 32 elements was performed by ICP-MS (Table 1). Detection limits for Zn and Au were 5 ppm and 1 ppb respectively. Mean concentrations of Au and Zn were 0.06 ppm and 1.15 wt.%, respectively.

Statistical analysis, geochemical modelling and ore evaluation of this prospect were conducted using *Micromine* software. After preparing the initial information and combining them in the *Micromine* software, 3D block models were produced for Zn and Au. The dimensions considered for modelling of each block was 10 × 10 × 5 m. Wireframe Zn was developed for concentrations greater than 3 and 5 wt.% individually. These concentrations were chosen based on the economic values at the mine.

Three-dimensional modelling of the Dagh Dali deposit for Au and Zn was performed using data from 49 borehole loops. The data from the sample analysis were transferred to specialized *Micromine* software in *Excel* format. By introducing the specification of each borehole to the software, the boreholes
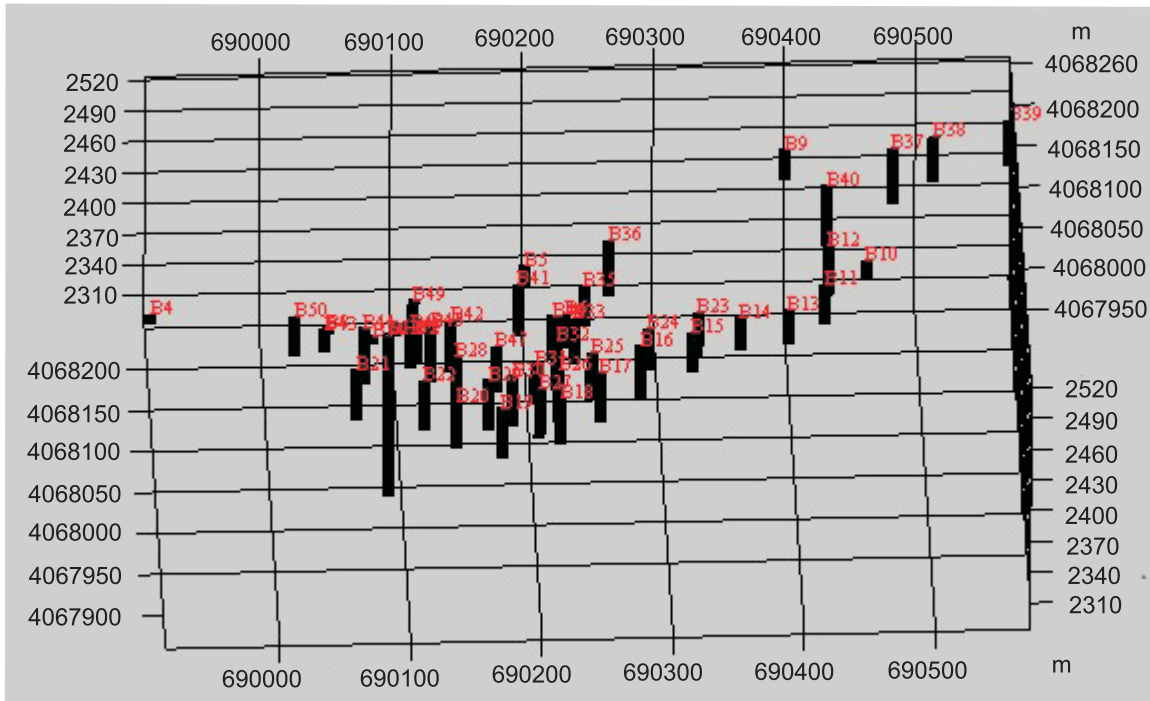
Fig. 3. Locations of boreholes in the Dagh Dali prospect

T a b l e   1

**Parameters of elements studied
in the Dagh Dali prospect**

Variable	Zn [%]	Au [ppm]
N	2196	2196
Mean	1.1514	0.0623
Median	0.32	0.03
Mode	0.12	0.02
Standard Deviation	2.68	0.082
Sample Variance	7.195	0.007
Kurtosis	42.76	16.12
Skewness	5.84	3.56
Range	28.32	0.6
Minimum	0	0
Maximum	28.32	0.59
Sum	2528.50	136.91

were defined in their in 3D spaces (Fig. 3). In order to prepare the volume model, a separate wireframe for each orebody was prepared as an empty shell and its volume was then calculated. The volumetric model was blocked into the dimensions of the ore deposit and then the concentration of each block was determined by the Ordinary kriging method.

To estimate the dispersion of Au and Zn in the Dagh Dali prospect, 2196 samples from 49 boreholes were modelled using the Ordinary Kriging geostatistical technique. Au concentrations ranged from 0 to 0.59 ppm and Zn showed a respective minimum and maximum concentration of 0 and of 28.32%. Borehole depths ranged from 7 to 160 m.

Kriging is a general approach that is used in a wide range of estimation methods, at a point or block, which depends on the least estimation error using the least-squares method. This term

was named by Matheron and Carlier in honour of Dr. Krige, an engineer who experimentally worked on stockpile estimates in several South African Au mines, after which the Earth theory was presented by Matheron (Sinclair and Blackwell, 2002). Kriging is an estimation method based on the weighted moving average which acts as the best linear unbiased estimator as used in ore grade estimation. In the best estimate, the variance value of the estimation error is minimal. Kriging is calculated based on the spatial correlation between the experimental data and the variogram function (Li and Heap, 2008). The ordinary kriging estimation equation is calculated as follows:

$$Z_V^* = \sum_{i=1}^n \lambda_t \cdot Z_{V_i} \qquad [1]$$

where: Z_V^* – estimated concentration, λ_i – weight or importance of the quantity of sample i and Z_{V_i} – concentration of sample i (Hasani Pak, 2003).

A variogram is a tool for determining the spatial correlation of a regionalized variable and it provides the required information on geological processes to determine anisotropy and different trends of formation (Marinoni, 2003):

$$\gamma(h) = \frac{1}{2n} \sum_{i=1}^n \left[Z(x_i) - Z(x_{i+h}) \right]^2 \qquad [2]$$

where: γ – empirical variogram and n is the number of pairs of points, $Z(x_i)$ – concentration at point x_i and $Z(x_{i+h})$ – concentration point at the h, distance from point x_i.

The variogram model simpliphies the linear estimation using the software, and its results are shown in a graph. Simple variograms must first be estimated and their model should be adapted to the spatial changes of random variables as a function of their separation distance (Antunes and Albuquerque, 2013). The stability or proper behaviour of the variogram model is a very

important preliminary step for geostatistical models (Leuangthong et al., 2011). In this research, the *Micromine* software was used to detect the mineralisation process and the dispersion of Au and Zn. An experimental variogram diagram is shown along with a fitted model for Au (Fig. 4). The variogram effect range is a very important parameter in selecting the search radius in the estimation process. As shown in Figure 4, Au has a 137 m radius of impact and a spherical variogram model. The experimental variogram and the fitted model for Zn with concentrations greater than 3 and 5% is illustrated in Figures 5 and 6, respectively. The variogram radius of impact is 3 on the 8% cutoff shape at 73 m and the 5% cutoff radius in Figure 6 is 69 m.

In this research, the concentration-volume fractal method is used to determine the mineral zone. The fractal and multi-particle fragmental models are based on the existence of a series of relationships between the power function of the index $M(\delta)$ and the variable δ in the region studied, which is as follows (Cheng and Li, 2002):

$$M(\delta) \propto \delta^{-\alpha} \qquad [3]$$

In equation [3], variable α is equal to the fractal dimension at each point of the logarithmic graph, which varies based on the multifractal nature of the geoscience data.

The power function $M(\delta)$ may be equal to the concentration, area, or volume of a concentration, including specific concentrations δ. The fractal model used by Afzal et al. (2011) for seperation of mineral zones in porphyry copper deposits is:

$$(\rho \le \nu) \propto \rho^{-\alpha 1}; (\ge \nu) \propto \rho^{-\alpha 2} \qquad [4]$$

where: ν indicates volume greater than, equal to, or smaller than ρ, $\alpha 2$ and $\alpha 1$ represent the fractal dimension at each point of the logarithmic graph and ρ represents the ore value (Sadeghi et al., 2012).

The threshold values in this model represent the boundaries of different mineralisation zones. To calculate ν in $(\rho \le \nu)$ and $(\rho \ge \nu)$, the volumes enclosed in the distance lines ρ in the three-dimensional model are used, together with the statistical estimates obtained from the results of chemical analysis of the mineral (Afzal et al., 2013).
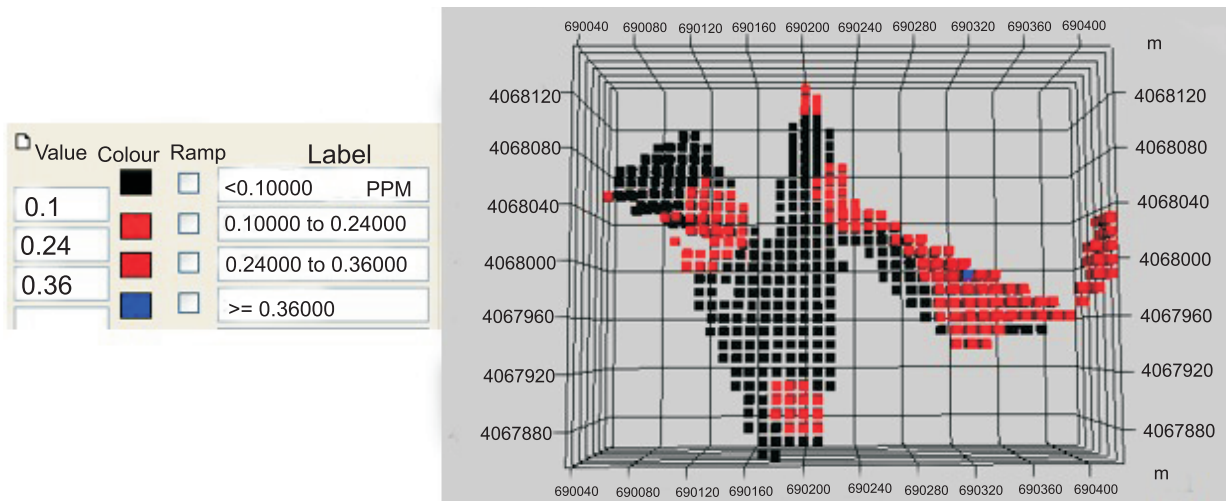

Fig. 4. Block model of Au concentration dispersion by the geostatistical method
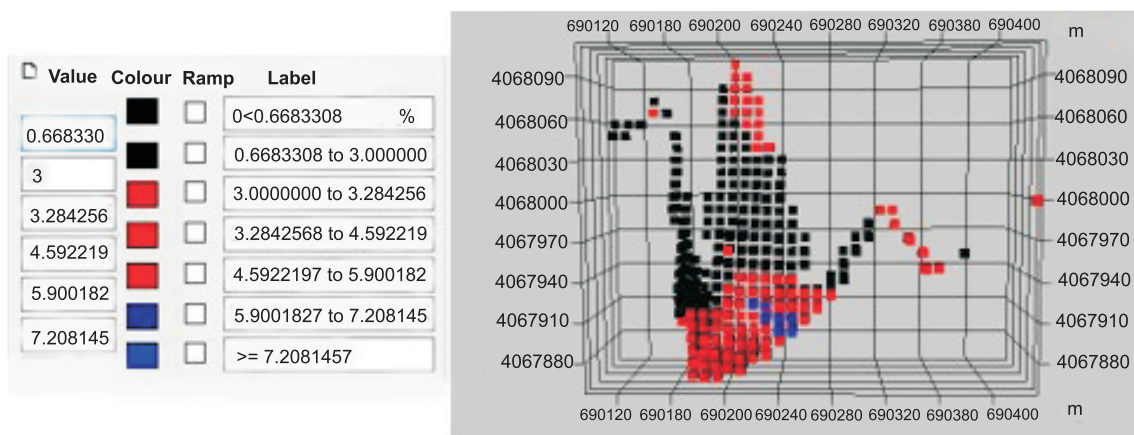

Fig. 5. Block model of Zn concentration dispersion >3% by the geostatistical method
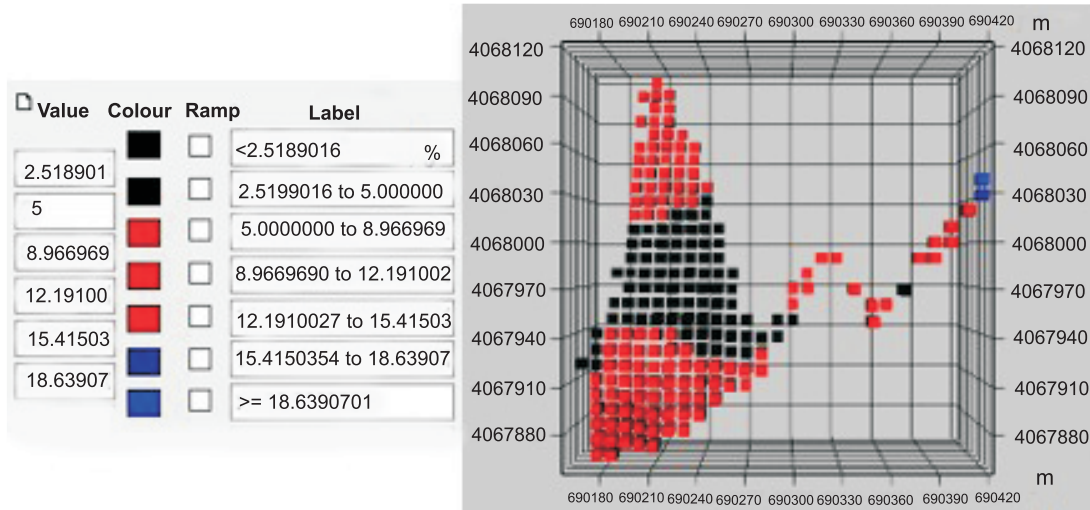
**Fig. 6. Block model of Zn concentration dispersion by >5%
by the geostatistical method**

DISCUSSION

By applying the C-V fractal method, high and low concentration ore zones can be distinguished. The advantage of the C-V fractal method is in drawing a fractal curve based on the size of each macro-block and its associated concentration, which ultimately leads to the differentiation of high-concentration streaks from low-concentration streaks (Afzal et al., 2011). To do this, the geochemical distributions of Au and Zn were first determined, using the ordinary Kriging geostatistics method.

The kriging standard errors were calculated for Zn and Au grades in blocks and the reserves were classified. The kriging estimator for a grade of each estimated block gives the value as a standard deviation of the estimate. This value is mostly a function of the geometrical position of the known data used to estimate the corresponding block grade. Depending on what level of confidence is needed, one can calculate the relative error of the block grade by multiplying a constant number, which is the function of the level of confidence, by the value of the standard deviation(s) and dividing the result by the number of samples (*n*) in each block's grade (*x*). Then by dividing the number obtained by the estimated value of the block and multiplying the number by 100, the percentage of relative error of the estimation of each block is obtained. These calculations are in accordance with equation [5]:

$$\%\text{Error} = \left(\frac{z \cdot s}{x\sqrt{N}}\right) \times 100 \qquad [5]$$

For a confidence level of 95%, this constant will be *z* = 1.96 and for 90% of confidence, *z* = 1.64. The kriging standard error for the gold and zinc elements is given in Table 2.

The block concentration distribution model of Au is shown in Figure 7, with the red and blue blocks having concentrations of >0.1 ppm while the black blocks have concentrations <0.1 ppm. Two different levels with concentrations >3 wt.% Zn and >5 wt.% Zn were created to obtain the economic range of the mine. The block concentration distribution models with concentrations higher than 3 and 5 wt.% are shown in Figures 8 and 9, respectively. In Figure 8, the concentration blocks with <3 wt.% are in black, between 3 and 5.9 wt.% are in red, and the concentration blocks >5.9 wt.% are in blue. In Figure 9, black, red and blue blocks represent concentrations of <5 wt.%, 5 to 15 wt.% and >15 wt.%, respectively.

In order to constrain the mineralisation process and the Au and Zn dispersion, a variogram was calculated using *Micromine* software. The empirical variogram diagram along with a fitted spherical model for Au is shown in Figure 4. As in Figure 5, the Au has a range of models of 91 m. The Zn empirical variogram along with the fitted model for concentrations >3 and >5 wt.% are shown in Figures 5 and 6, respectively. The range of the model

Table 2

Kriging standard errors for Au and Zn

| Kriging standard error					
Confidence level	Element	Error <10%	10%<Error<30%	30%<Error<50%	Error<50%
95%	Au	26 075 tons (Ave Au 0.23ppm)	347 375 tons (Ave Au 0.15 ppm)	192 325 tons (Ave Au 0.2 ppm)	250 425 tons (Ave Au 0.15 ppm)
95%	Zn3%	7 218.75 tons (Ave Zn 3% 5.7 ppm)	167 234.4 tons (Ave Zn 3% 3.4 ppm)	76 140.63 tons (Ave Zn 3% 3 ppm)	103 812.5 tons (Ave Zn 3% 2.7 ppm)
95%	Zn5%	7 218.75 tons (Ave Zn 5% 7.6 ppm)	183 046.9 tons (Ave Zn 5% 5.1 ppm)	46 234.38 tons (Ave Zn 5% 5.6 ppm)	68 750 tons (Ave Zn 5% 5.3 ppm)
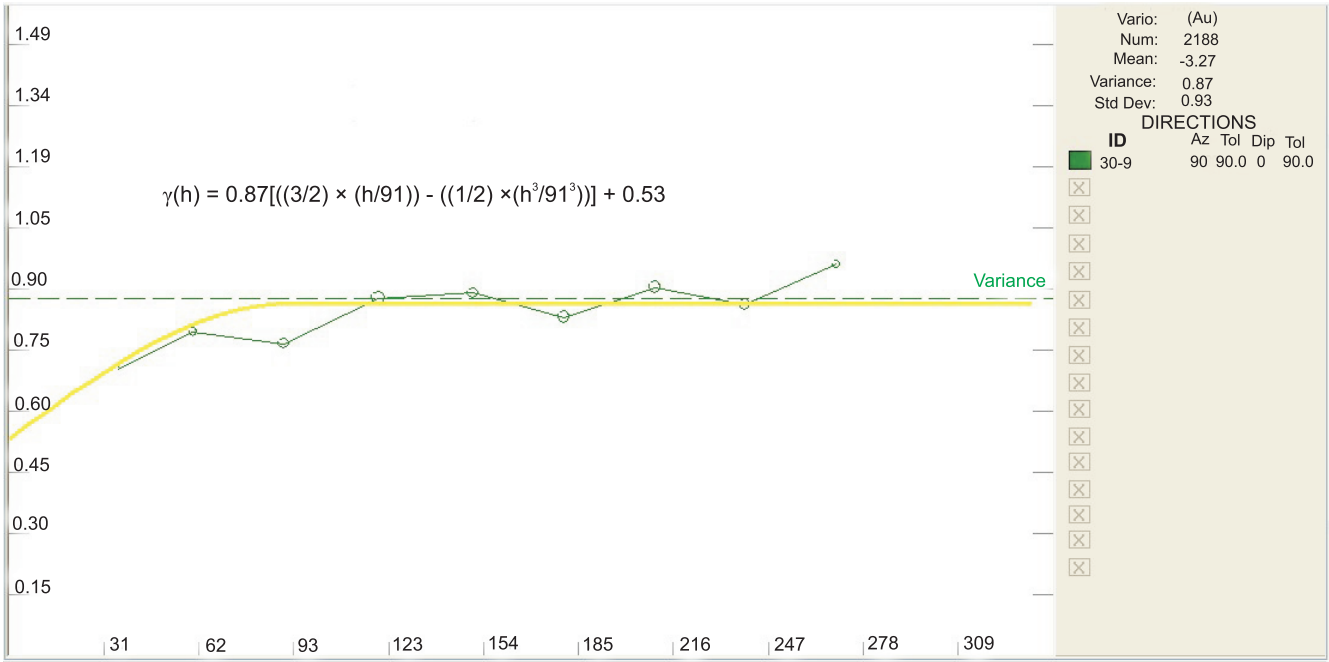
Fig. 7. Experimental variogram with a fitting model for the distribution of Au
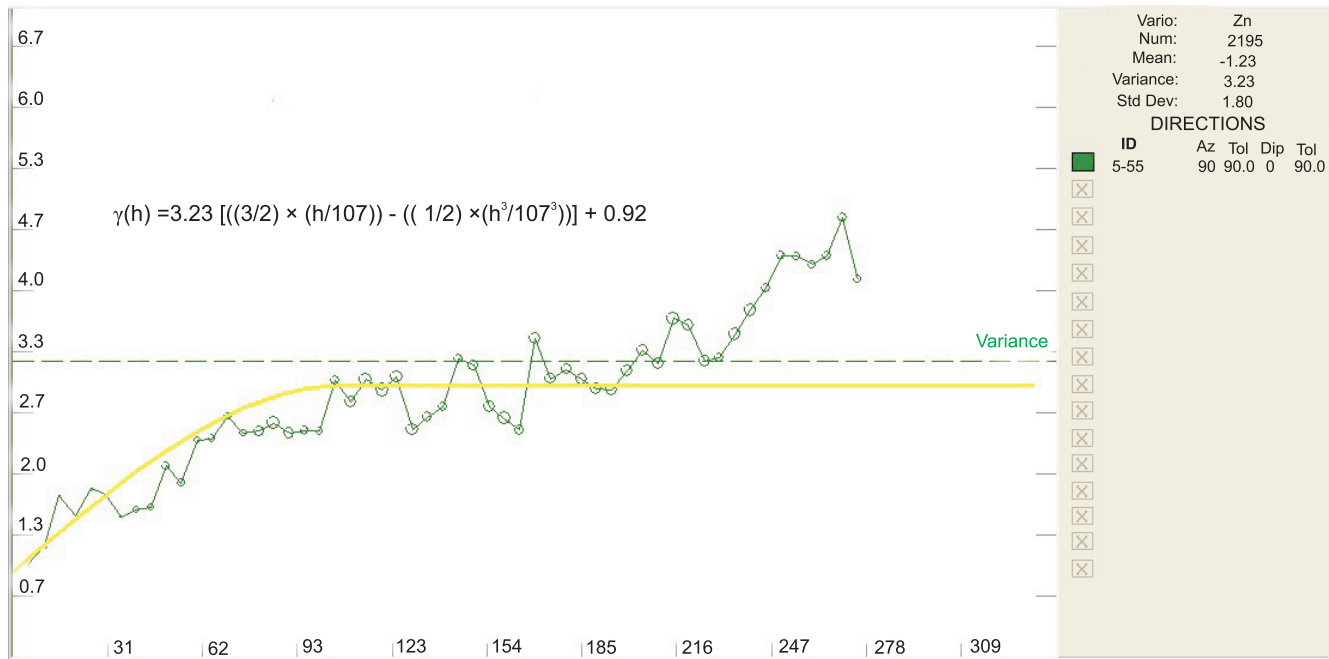

Fig. 8. Empirical variogram along with a fitted model for Zn for wireframe concentrations of >3%

for 3 wt.% Zn concentration in Figure 8 is 107 m and the range of the model for 5 wt.% Zn concentration in Figure 9 is 121 m.

Finally, the C-V fractal method was used to determine the mineralisation zone based on the concentration indices. Considering the fact that the volume of each micro-block is known and the concentration value of each element is calculated for each micro-block, the concentration of each element was first arranged in descending order, then the volume of each concentration block was calculated according to the dimensions of the blocks. The concentration logarithm of each element and the cumulative volume were captured and the logarithmic concentration-volume graph was plotted.

An exponential relationship was found between concentration and the cumulative volume contained therein. Relationship between the change in concentration and the volume containing the lower concentrations is shown in the logarithmic diagram of Figure 10. Since the concentration of each element, as shown in Figure 10, is a part of the logarithmic diagram in a Zn range with a concentration of >5 wt.%, the following relation was found with a volume concentration <5 wt.%:

$$\gamma(h) = 3.23[((3/2) \times (h/121)) - ((1/2) \times (h^3/121^3))] + 0.93$$
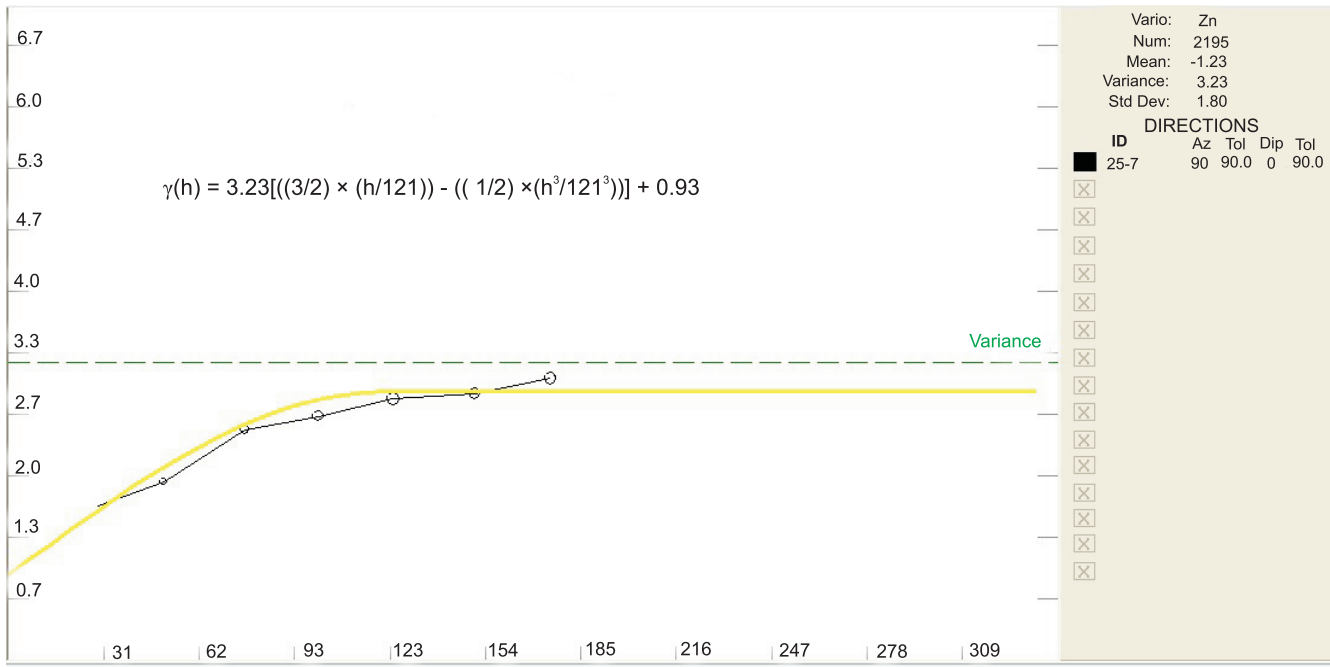
Fig. 9. Experimental variogram along with a fitted model for Zn for wireframe concentrations of >5%

$$V(T) - V(\rho) = C\rho^{-\beta} \quad [6]$$

where: $V(T)$ is equal to the sum of the volume of all divided sub-blocks and $V(\rho)$ is equal to the volume containing concentration ń and concentrations greater than that.

The linear wall rock equation for Zn values in the range of 5 wt.% is given by [7].

$$y = -1.0384x + 5.4908 \quad [7]$$

were: x and y are log ρ and log $V(\geq\rho)$, respectively;

therefore:

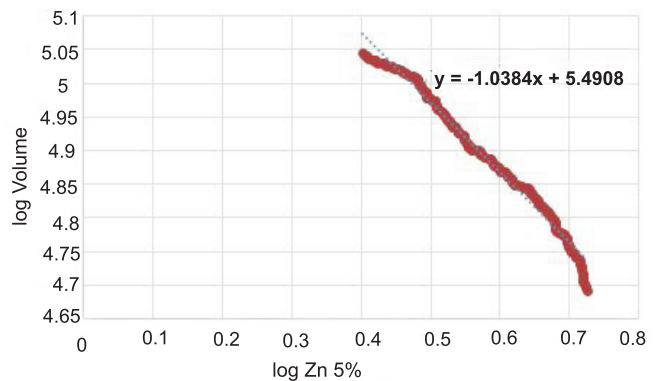$$\log V(\geq\rho) = -1.0384\log \rho + 5.4908 \quad [8]$$

With simplification we will have:

$$\log V(\geq\rho) = \log \rho^{-1.0384} + \log^{105.4908} \quad [9]$$

$$\log V(\geq\rho) = \log (10^{5.4908} \times \rho^{-1.0384}) \quad [10]$$

And from this equation, the relationship between volume and concentration would be as follows:

$$V(\geq\rho) = 10^{5.4908} \times \rho^{-1.0384} \quad [11]$$

Fig. 10. Logarithmic curve showing the relationship between concentration and volume containing concentrations <5% Zn

According to equation [4], the dimension of this line is 1.0384 where ρ is equal to concentration and $V(\geq\rho)$ is equal to the volume containing the concentration and concentrations higher than this value. Considering the success of fractal methods in two dimensions including the method of concentration-area and method of concentration-number, it can be concluded that the fractal method is more complex in three dimensions and it is thus more efficient. Using these methods, low concentration and high concentration mineralisation can be identified. The sharp change in the curve slope in the logarithmic concentration-volume graph indicates the change in the
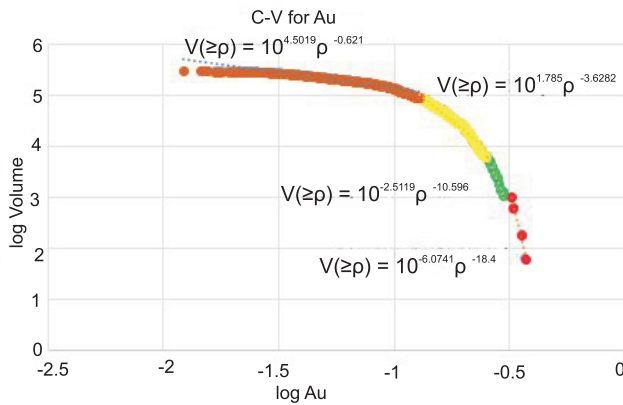
C-V for Au

$$V(\geq\rho) = 10^{4.5019}\rho^{-0.621}$$

$$V(\geq\rho) = 10^{1.785}\rho^{-3.6282}$$

$$V(\geq\rho) = 10^{-2.5119}\rho^{-10.596}$$

$$V(\geq\rho) = 10^{-6.0741}\rho^{-18.4}$$

Fig. 11. Logarithmic curve of concentration – volume for Au in the range of the Dagh Dali

C-V for Zn 3%

$$V(\geq\rho) = 10^{5.1506}\rho^{-0.6965}$$

$$V(\geq\rho) = 10^{7.7669}\rho^{-5.275}$$

$$V(\geq\rho) = 10^{12.208}\rho^{-11.235}$$

$$V(\geq\rho) = 10^{15.805}\rho^{-15.902}$$
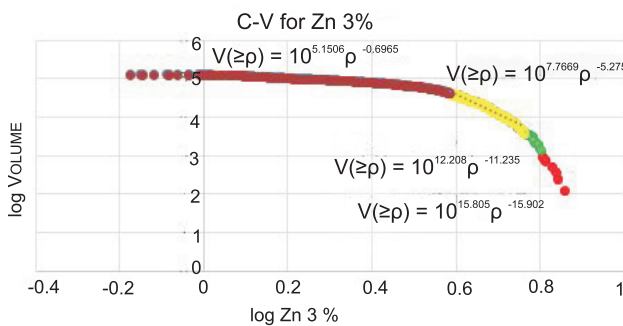
Fig. 12. Logarithmic curve of concentration – volume for Zn with wireframe concentrations of >3%

concentration community from the surrounding areas to the ore-bearing area. The logarithmic concentration-volume curve for Au is shown in Figure 11. This curve clearly shows 4 distinct communities and 3 failure points. These three breaking points correspond to concentrations of 0.12, 0.26 and 0.31 ppm, respectively. The logarithmic concentration-volume curve for Zn with values of 3 and 5% is shown in Figures 12 and 13, respectively. In Figure 12, which refers to Zn with wireframe values of >3 wt.%, there are four populations and three failure points. These breakpoints correspond to concentrations of 3.80, 5.75, and 6.30 wt.% for Zn. Based on these breakpoints and concentration communities, four zones with concentration ranges of <3.80 wt.%, 3.80–5.75 wt.%, 5.75–6.30 wt.%, and a cut-off concentration of >6.30 wt.% can be separated with regard to an extraction factor of 3 wt.% Zn.

Based on the extraction factors, three zones can be recognized: a zone with grade less than the cut-off grade (concentrations <3.80 wt.% Zn), an ore zone (concentration range 3.80–6.30 wt.% Zn), and a high concentration zone (concentrations >6.30 wt.% Zn). In terms of the extraction factor, these three zones can be considered as a zone of with less than concentration limits (concentration range <3.80 wt.% Zn), a mineral zone

(concentration range 3.80–6.30 wt.% Zn), and a high concentration zone (concentration range >6.30 wt.% Zn).

There are also three breakpoints in Figure 13, which correspond to wireframe values of >5 wt.%. However, the concentration values of these breakpoints differ from the concentration values of the breakpoints in Figure 12, as these are related to concentrations of 5.37, 10.47 and 17.8 wt.% of Zn. Based on this graph, the extractable ore can be considered in the concentration range of 5.37–17.78 wt.% of Zn. A concentration range of >17.78 wt.% can also be separated as a high concentration zone. The concentration range of <5.37 wt.% is suggested to be the host rock. The different concentration zones classified based on the concentration-volume fractal graphs for Au and Zn, are shown in Table 3. The block model for Au is shown in Figure 14 and the block models for Zn are illustrated in Figures 15 and 16.

In the block model for Au (Fig. 14), concentrations of >0.12 ppm are shown in red and blue colours while black represents concentrations of <0.12 ppm. In Figure 15, the concentration of <3.80 wt.% is shown in black while red and blue colours indicate concentrations between 3.80 and 6.30 and >6.30 wt.%. In Figure 16, concentrations of <5.37 wt.% are in black and concentrations between 5.37 and 17.78 and >17.78 wt.% are in red and blue, respectively.
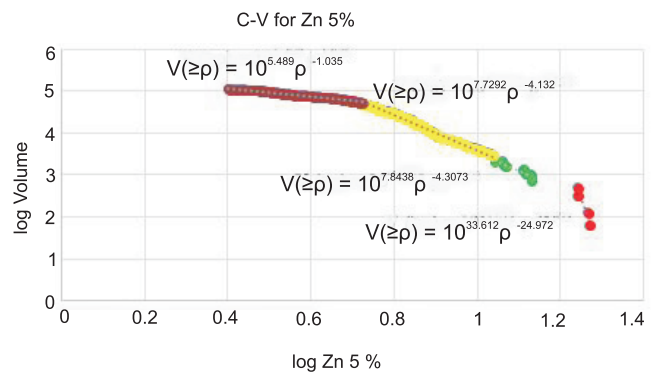
C-V for Zn 5%

$$V(\geq\rho) = 10^{5.489}\rho^{-1.035}$$

$$V(\geq\rho) = 10^{7.7292}\rho^{-4.132}$$

$$V(\geq\rho) = 10^{7.8438}\rho^{-4.3073}$$

$$V(\geq\rho) = 10^{33.612}\rho^{-24.972}$$

Fig. 13. Logarithmic curve of concentration – volume for Zn with wireframe concentrations of >5%

Table 3

Concentration of Au and Zn communities based on the fractal concentration-volume method

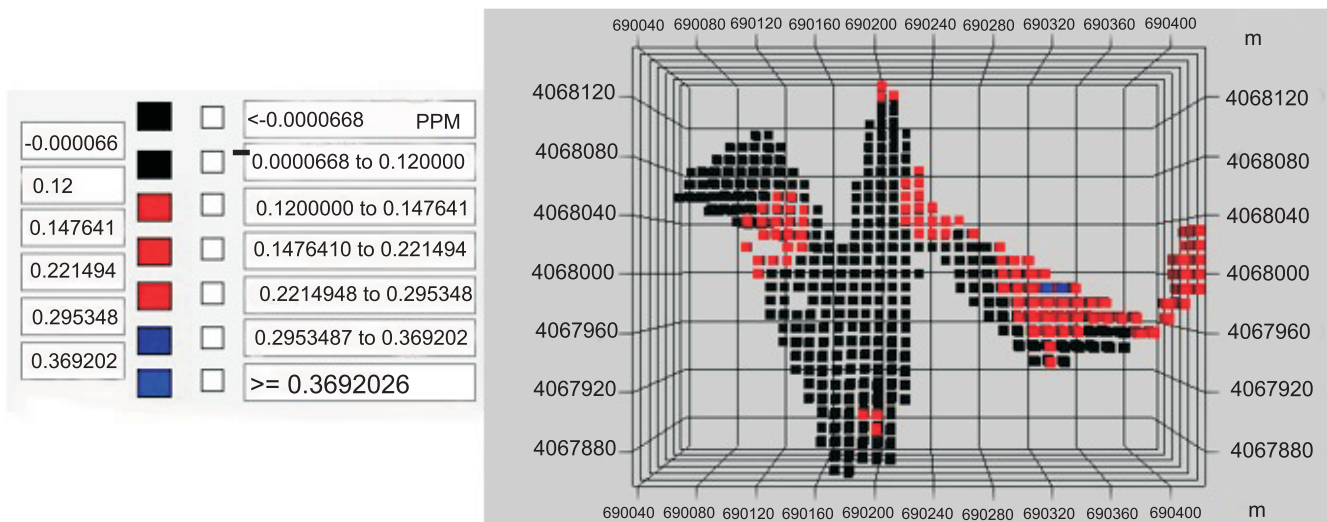| Concentration community	Wall rock	Low concentration zone	High concentration zone	Enriched zone
Au threshold [ppm]	−	0.12	0.26	0.31
Au concentration range [ppm]	<0.12	0.12–0.26	0.26–0.31	>0.31
3% Zn threshold	−	3.80	5.75	6.30
3% Zn concentration range	<3.80	3.80–5.75	5.75–6.30	>6.30
5% Zn threshold	−	5.37	10.47	17.78
5% Zn concentration range	<5.37	5.37–10.47	10.47–17.78	>17.78

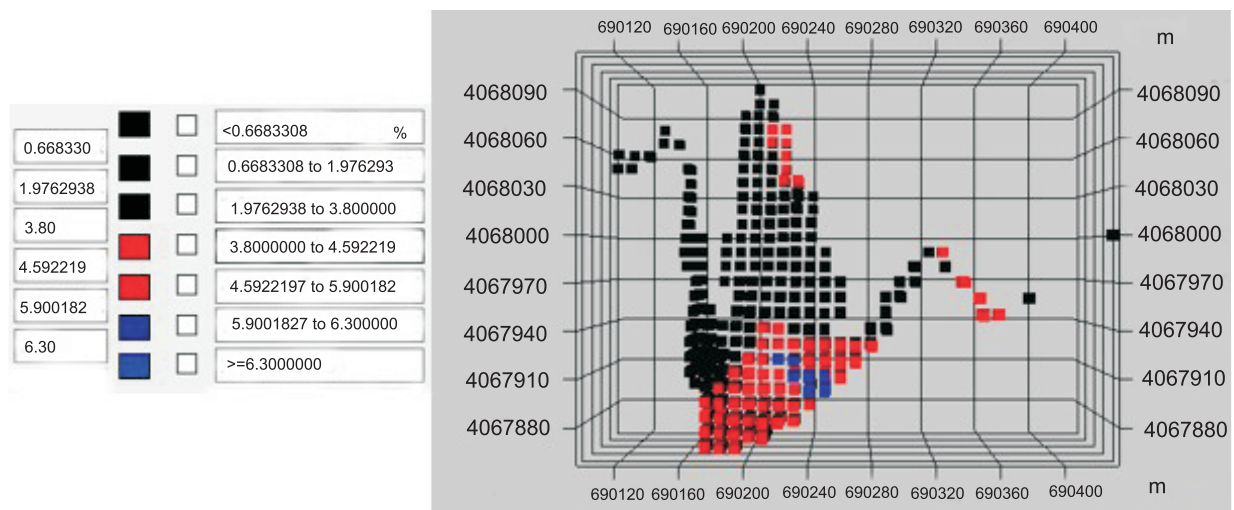**Fig. 14. Au block model derived from the concentration-volume method**

Fig. 15. Block model for Zn Wireframe >3% up from the concentration-volume method

CONCLUSIONS

Fractal methods can be very useful not only at the surface but also in volume and in subsurface studies. Traditional methods are based on lithological and mineralogical studies and hence are time-consuming and costly. In this research, the distribution of element concentrations was compared using a geostatistical method and fractal modelling in the exploration area of Dagh Dali. Based on this comparison, ore blocks with high concentrations were determined for each element and the approximate boundary for each zone was determined. With the information obtained, the volume of each block and its concentration were determined. The concentration-volume graph was

plotted and the concentration communities were determined based on the points of failure of these curves for Au and Zn. These concentration communities can be attributed to low concentration, high concentration, enriched, and wall rocks. With respect to Au, the 0.31 ppm zone coincides with enriched concentration, which has a small amount of reserve, and it can be concluded that the mineralisation of Au has a small tonnage: it seems that the Dagh Dali prospect does not have economic potential for Au. Nevertheless, Pouya Zarkanagh Agh Darreh, which operates the Agh Darreh Au deposit, is currently considering the cut-off concentration of Au for this mine at 0.1 ppm. Hence, the Dagh Dali exploration prospect can be profitable for this company. Zn has economic potential due to blocks with economic concentrations. The concentration block model
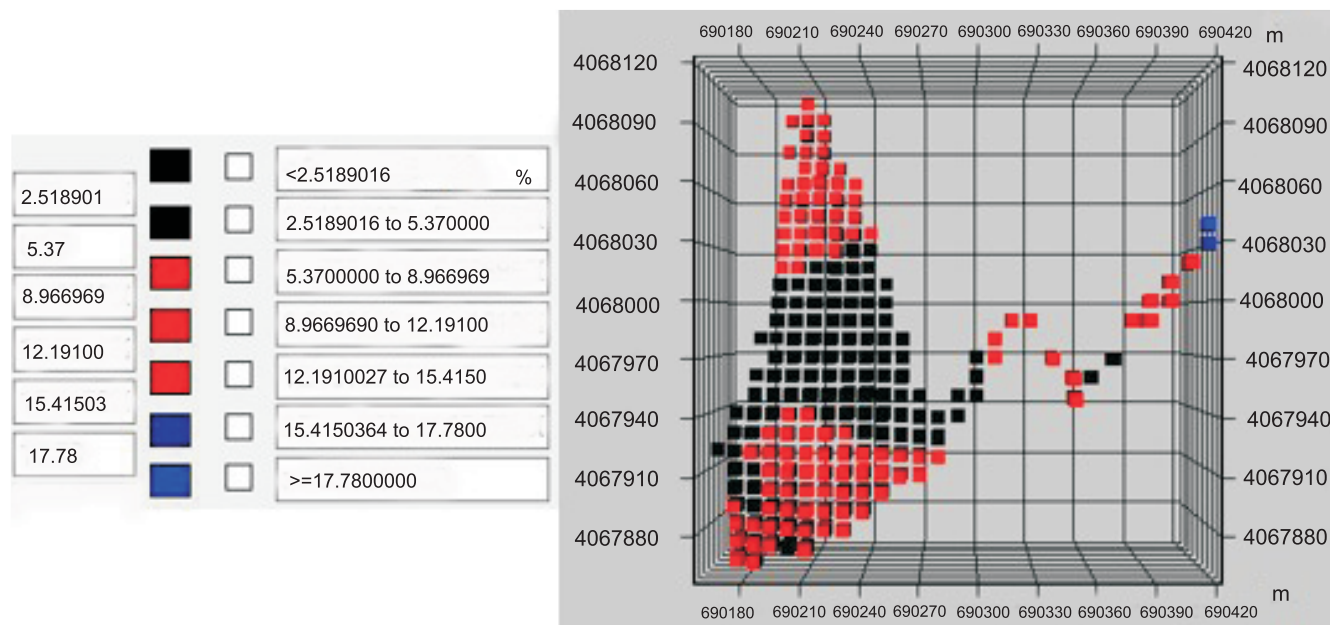
Fig. 16. Block model for Zn Wireframe >5% up from the concentration-volume method

adapted from the fractal method is consistent with the geostatistical method, but the deposit showed a volume smaller than the volume obtained by geostatistical methods. The amount of Zn deposit for the >3 wt.% concentration range by using the geostatistical method is 350,996 tons with a mean concentration of 3.13 wt.%, while the concentration-volume fractal method gives a reserve of 119,532 tons for concentrations >3.80 wt.%; also, the reserves for the concentrations >5 wt.% using the geostatistical method is 303,685 tons with average concentration of 5.29 wt.%, and for the concentration-volume fractal method, the reserve is 128,981 tons for 5.37 wt.% and more.

REFERENCES

Afzal, P., Dadashzadeh, H., Rashidnejad, N., Aliyari, F., 2013. Delineation of Au mineralized zones using concentration – volume fractal model in Qolqoleh Au deposit, NW Iran. Ore Geology Reviews, **55**: 125–133.

Afzal, P., Fadakar, Y., Khakzad, A., Moarefvand, P., Rashidnejad, N., 2011. Delineation of mineralization zones in porphyry Cu deposits by fractal concentration – volume modeling. Journal of Geochemical Exploration, **108**: 220–232.

Afzal, P., Khakzad, A., Moarefvand, P., Rashidnejad, N., Esfandiari, B., Fadakar, Y., 2010. Geochemical anomaly separation by multifractal modeling in Kahang (Gor Gor) porphyry system,Central Iran. Journal of Geochemical Exploration, **104**: 34–46.

Alavi, M., Hajian, J., Amidi, M., Bolourchi, H., 1982. Geology of the Takab-Saein-Qal'eh. Geol. Surv. Iran. Rpt 50.

Alavi, M., 1994. Tectonics of the Zagros orogenic belt of Iran: new data and interpretations. Tectonophysics, **229**: 211–238.

Antunes, I.M.H.R., Albuquerque, M.T.D., 2013. Science of the total environment using indicator kriging for the evaluation of arsenic potential contamination in an abandoned mining area (Portugal). Science of the Total Environment, **442**: 545–552.

Asadi, H.H., Hale, M., 1999. Magmatic contribution to the Carlin-type Au deposit at Zarshuran, Iran. Proceedings of the Fifth Joint SGA-IAGOD International Meeting, Imperial College, London.

Asadi, H.H., Hale, M., 2001. A predictive GIS model for mapping potential Au and base metal mineralization in Takab area, Iran. Computers and Geosciences, **8**: 901–912.

Bai, J., Porwal, A., Hart, C., Ford, A., Yu, L., 2010. Mapping geochemical singularity using multifractal analysis: application to anomaly definition on stream sediment data from Funin Sheet, Yunnan, China. Journal of Geochemical Exploration, **104**: 1–11.

Carranza, E.J., 2008. Geochemical Anomaly and Mineral Prospectivity Mapping in GIS. Handbook of Exploration and Environmental Geochemistry, Elsevier.

Carranza, E.J.M., 2009. Controls on mineral deposit occurrence inferred from analysis of their spatial pattern and spatial association with geological features. Ore Geology Reviews, **35**: 383–400.

Carranza, E.J.M., Owusu, E.A., Hale, M., 2009. Mapping of prospectivity and estimation of a number of undiscovered prospects for lode Au, southwestern Ashanti Belt, Ghana. Mineralium Deposita, **44**: 915–938.

Carranza, M., Sadeghi, M., 2010. Predictive mapping of prospectivity and quantitative estimation of undiscovered VMS deposits in Skellefte district (Sweden). Ore Geology Reviews, **38**: 219–241.

Cheng, Q., 1999. Spatial and scaling modeling for geochemical anomaly separation. Journal of Geochemical Exploration, **65**: 175–194.

Cheng, Q., 2007. Mapping singularities with stream sediment geochemical data for prediction of undiscovered mineral deposits in Gejiu, Yunnan Province China. Ore Geology Reviews, **32**: 314–324.

Cheng, Q., Li, Q., 2002. A fractal concentration – area method for assigning a color palette for image representation. Computers and Geosciences, **28**: 567–575.

Cheng, Q., Agterberg, F.P., Ballantyne, S.B., 1994. The separation of geochemical anomalies from the background by fractal methods. Journal of Geochemical Exploration, **2**: 42–67.

Cheng, Q., Ping, Q., Kenny, F., 1997. Statistical and fractal analysis of surface stream patterns in the Oak Ridges Moraine, Ontario, Canada. International Association of Mathematical Geology Meeting, Barcelona, Spain.

Daliran, F., 2003. Discovery of 1.2 kg/t gold and 1.9 kg/t silver in mud precipitates of a cold spring from the Takab geothermal field, NW Iran. Mineral exploration and sustainable development: 461–464.

Daliran, F., 2008. The carbonate rock-hosted epithermal Au deposit of Agdarreh, Takab geothermal field, NW Iran – hydrothermal alteration and mineralization. Mineralium Deposita, **43**: 383–404.

Davis, J.C., 2002. Statistics and Data Analysis in Geology. John Wiley and Sons.

Ghorbani, M., 2013. The Economic Geology of Iran. Springer.

Gonçalves, M.A., Mateus, A., Oliveira, V., 2001. Geochemical anomaly separation by multifractal modelling. Journal of Geochemical Exploration, **72**: 91–114.

Hasani Pak, A.A., 2003. Geostatistics. Tehran University Press.

Karimi, M.,1993. Petrographic-mineralogical studies, and the genesis of the Au-As ore at Zarshouran (Takab) (in Persian with English abstract). M.Sc. thesis, University of Tarbiat Moallem, Tehran.

Leuangthong, O., Khan, K.D., Deutsch, C.V., 2011. Solved Problems in Geostatistics, John Wiley and Sons.

Li, Ch., Ma, T., Shi, J., 2003. Application of a fractal method relating concentrations and distances for separation of geochemical anomalies from the background. Journal of Geochemical Exploration, **77**: 167–175.

Li, J., Heap, A.D., 2008. A Review of spatial interpolation methods for environmental scientists. Geoscience Australia: 137–145.

Lowell, J.D., Guilbert, J.M., 1970. Lateral and vertical alteration-mineralization zoning in porphyry ore deposits. Economic Geology, **65**: 373–408.

Mandelbrot, B.B., 1983. The Fractal Geometry of Nature. W.H. Freeman and Company New York.

Marinoni, O., 2003. Improving geological models using a combined ordinary – indicator kriging approach. Engineering Geology, **69**: 37–45.

Rahimsouri, Y., Mehrabi, B., Alipour, Sh., 2019. Mineralogy, geochemistry and fluid inclusion studies of Dagh-Dali Zn-Pb(±Au) Deposit, Northern Takab, Northwest Iran (in Persian). Iranian Journal of Petrology, **35**: 217–244.

Sadeghi, B., Moarefvand, P., Afzal, P., Bijan, A., Daneshvar, L., 2012. Application of fractal models to outline mineralized zones in the Zaghia iron ore deposit, Central Iran. Journal of Geochemical Exploration, **122**: 9–19.

Sim, L., Bankwitz, P., Korcemagin, V.A., Frischbutter, A., 1999. The neotectonic stress field pattern of the East European Platform. Zeitschrift fur Geologische Wissenschaften, **27**: 161–182.

Sinclair, A.J., Blackwell, G.H., 2002. Applied Mineral Inventory Estimation. Cambridge University Press.

Stöcklin, J., 1968. Structural history and tectonics of Iran: a review. AAPG Bulletin, **52**: 1229–1258.

Zuo, R., Cheng, Q., Xia, Q., 2009. Application of fractal models to the characterization of vertical distribution of geochemical element concentration. Journal of Geochemical Exploration, **102**: 37–43.